



Original paper

Adsorption of cationic dye from aqueous solution using SBA-15 nano particles synthesized by stem sweep ash as the source of silica

Elham Chiani¹, Seyed Naser Azizi^{1,*}, Shahram Ghasemi², Salma Ehsani Tilami³

¹Department of Analytical Chemistry, Faculty of Chemistry, University of Mazandaran, Babolsar, Iran.

²Department of Nano, Faculty of Chemistry, University of Mazandaran, Babolsar, Iran.

³Department of Basic Science, Farhangian University, Tehran, Iran.

GRAPHICAL ABSTRACT



ARTICLE INFO

Article history:

Received 20 August 2020

Reviewed 16 October 2020

Received in revised form 20 December 2020

Accepted 21 December 2020

Keywords:

Stem sweep ash

Azure B

Nano particles

SBA-15

ABSTRACT

Today, many efforts have been made to use agricultural waste as a cheap and abundant resource for providing suitable adsorbents to remove pollutants such as industrial dyes. The aim of this study was to remove dye from water under different conditions using SBA-15 nano particles as adsorbents their silica was prepared from stem sweep ash (SSA). Fourier transform infrared spectroscopy (FTIR), scanning electron microscope (SEM), transmission electron microscope (TEM), X-ray diffraction (XRD) and N₂ adsorption experiments were applied to evaluate the structural characteristics of obtained adsorbent. In addition, to remove Azure B dye by SBA-15, the optimal values were obtained as the parameters of contact time = 30 min, pH = 8, temperature = 65 °C, adsorbent amount = 0.01 g, stirring rate = 90 rpm and initial dye concentration = 100 mg/L. The kinetic and thermodynamic experiments were conducted on the adsorption process as well. The results of the experiments demonstrated that the total surface area and total pore volume of the adsorbent were 780 m²/g and 0.8483 cm³/g, respectively. Moreover, the surface adsorption process of Azure B followed the Langmuir's isothermal model, and kinetic data followed the surface adsorption of pseudo-second-order kinetic model. Besides, the values of ΔH° and ΔS° were 5409.32 J/mol and 37.28 J/mol K, respectively, and the maximum adsorption capacity of adsorbent was 166.66 mg/g.

©2020 Razi University-All rights reserved.

1. Introduction

Textile and dyeing industries are one of the industries that should pay special attention to the treatment of their effluents (Daneshvar et al. 2003). The textile industries produce effluents containing various chemicals which are poisonous, resistant to biodegradation and stable

*Corresponding author Email: seyednaserazizi@yahoo.com

in the environment (Muhammad et al. 2008). Dyes as organic compounds are widely applied in numerous industries including textile, tannery and paper (Abo-Farha. 2010). Among the available dyes, about 60-70 % of the dyes used in the dyeing process are azo-reactive ones, and about 10-50 % of these dyes enter into wastewater due to the relatively low stabilization efficiency compared to other dyes

(Kyzas. 2012). Reactive poisonous dyes are mutagenic and resistant to biological treatment, and their discharge into ecosystems has increased environmental risks (Belessi et al. 2009). These dyes are water-soluble and resistant to light and chemical agents as well as are not easily removed by conventional treatment technique (Gök et al. 2010). Therefore, the management of reactive dye-containing wastewater is very important.

Different methods including adsorption, photo catalysis as well as membrane and electrochemical processes have been used to remove organic pollutants from wastewaters. Among these methods, adsorption is a great way to improve the quality of the wastewater. Its advantages over traditional processes are its cost-effectiveness, ease of use and high ability to remove dyes (Lotito et al. 2014).

In recent years, many studies have been conducted to find economical and effective adsorbents. Zeolites and porous silica materials which can be restored by preserving their original properties are one of the best adsorbents used in the process of removing dyes and heavy metals (Ghadiri et al. 2010).

The silicon source in silicate compounds can be supplied from sodium silicate, silica gel, silicic acid, colloidal silica and amorphous solid silica (Kikuchi. 1999). Among the siliceous natural resources, the use of cheap stem sweep ash (SSA) in the preparation of silica powder and synthesis of zeolites for photo catalytic, isolation and petrochemical processes has also been reported (Thuadajj and Nuntiya. 2008).

In 1998, a new family of regular mesoporous silica materials synthesized with high-density polyethylene and polypropylene oxides in acidic conditions using non-ionic copolymers was reported as well as it was mentioned that the tetraethoxysilane and tetramethoxysilane were used as a source of silica (Ulrich et al. 2010). Since then, among these silicate materials, SBA-15, next SBA-16 have been rapidly taken into account because of the desirable surface physicochemical properties such as low toxicity, biocompatibility and biodegradability, and this family is now the focus of attention for studies (Speybroeck et al. 2008).

The use of natural materials and resources in the synthesis of chemical compounds is very important in terms of cost and environmental issues and the use of materials for various usages such as the methods for the remediation and treatment of commercial textile dyes present in textile wastewater has been rapidly developed in recent years.

Agricultural waste such as sweep (sorghum) has little economic value and is unpleasant for the environment, and converting agricultural waste to silica in silicate materials can be a good solution to solve environmental problems for their consumption as well as to produce silica and cheap silicate materials (Azizi et al. 2014).

Therefore, the aim of this study was to assess the ability of synthesized mesoporous SBA-15 with natural silica source of SSA for adsorption of Azure B dye. To do so, factors affecting the adsorption phenomena including ambient pH, initial concentration of adsorbent, contact time, adsorbent amount, stirring rate and temperature were evaluated, too. The innovation of the current study is the use of agricultural waste like stem sweep as a cheap and abundant silica source to synthesize the SBA-15 and utilize this suitable adsorbent for removing Azure B industrial dye from aqueous solutions at a lower cost.

2. Experimental

2.1. Chemicals

To synthesize the mesoporous SBA-15 and perform dye adsorption test, the sweep (sorghum) stem was provided from sweep fields in Mazandaran, Iran. NaOH (98 %) and H₃PO₄ were purchased from Merck and EO20-PO70-EO20 (Mav=5800) from Aldrich Company. Ethylene Azure B was obtained from the company of Fluka according to molecular formula: C₁₅H₁₆ClN₃S, molar mass: 305.824 g/mol and purity degree: 99 %. The chemical structure of the dye is shown in Fig. 1. All solutions were prepared using distilled water.

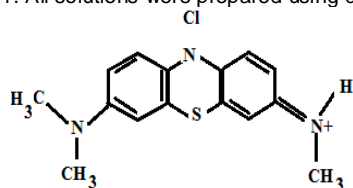


Fig. 1. Chemical structure of the Azure B dye.

2.2. Preparation of mesoporous SBA-15 particles

In the preparation of mesoporous SBA-15 particles, the SSA was used as a source (Kalapathy et al. 2000). For this purpose, some sweep stems were first burnt to obtain the ash. Then, the SSA was treated with 1 mol of HCl for 5 hours and was calcined in an electric furnace at 600 °C. The 2.75 g calcined white ash was dissolved 2 mol/L NaOH at 50 °C, and the required silica solution formed the synthesis of the mesoporous SBA-15 particles. Similarly, synthesis of mesoporous SBA-15 was conducted based on our previous published paper (Azizi et al. 2013). In a synthesis of sample, 3 g of P123 copolymer was dissolved 85 % H₃PO₄ solution at 40 °C in an oil bath under stirring. The prepared silicate alkaline solution was immediately added to this solution. Then, 1.84 g of H₃PO₄ was dissolved 5 mL water and added to the above solution, and the final volume of distilled water was reached to 80 mL. After mixing the solution for 2 minutes, the obtained gel was transferred to a polypropylene container and placed in oil bath at 40 °C for 48 hours. The prepared material was filtered, dried at 70 °C after washing with distilled water and finally was calcined for 5 hours at 250 °C and for 3 hours at 550 °C.

Although, at this stage, due to the fact that there are different methods such as calcination, solvent extraction, ozone oxidation method and so on (Xiao et al. 2006), complete elimination of template occurs based in calcination method on research (Xiangping et al. 2019). For this reason, in the current study, it has been given priority over other methods.

2.3. Characterization of SBA-15 particles

Detection and characterization of synthesized SBA-15 were performed in the step-scanning mode 2θ using an X-ray diffraction (XRD) pattern and an X-ray diffractometer (GBC, MMA) with Cu Kα (λ = 1.5418 Å) and the scanning speed of 5°/min. The framework vibrations of mesoporous SBA-15 were recorded on a FT-IR spectrophotometer (Bruker-Vector), in the range of 500-3500 cm⁻¹ using KBr pellet. Moreover, evaluating the surface morphology and structure of synthesized samples was carried out using Scanning electron microscopy (FE-SEM; model Hitachi, S-4160). The samples' special surface area was delineated based on the linear portion of the Brumauer-Emmet-Teller (BET, model BELSORP mini 100 instruments) plots. The conventional Barret-Joyner-Halenda (BJH) method was applied to compute the pore size (diameter DBET) distribution according to the nitrogen adsorption data. In addition, and Transmission electron microscope (TEM) investigations of synthesized SBA-15 were performed on Philips CM10 instrument at an acceleration voltage of 100 kV.

2.4. Adsorption experiments

2.4.1. Preparation of dye samples

The stock solution at a concentration of 500 mg/L was prepared via dissolving 0.5 g Azure B in one liter of distilled water. Experimental solutions with different concentrations were obtained through diluting the stock solution. Dye adsorption experiments were done to determine the effect of important parameters like contact time, pH, concentration, adsorbent amount and stirring rate of solution on removal of cationic Azure B. In this method, 25 mL of dye solution with certain concentration (100 mg/L) and initial pH of 5.5 were mixed with 0.01 g of mesoporous SBA-15 and stirred at a constant speed of 150 rpm in a rotary shaker.

Samples were centrifuged for 15 minutes at different intervals in a centrifuge machine at 14000 rpm, and the adsorption amount of the filtered solutions was measured to determine the concentration of remaining dye using UV-Vis at a wavelength of 648 nm for Azure B. The amount of dye adsorbed onto the adsorbent at equilibrium, q_e (mg/g) was calculated by the following formula:

$$q_e = (C_0 - C_e)/w \quad (1)$$

where, C_e and C₀ are the equilibrium and initial dye concentrations in mg/L respectively. W indicates the amount of adsorbent (g) and V illustrates the volume of solution (L). The percentage of dye removal was obtained by the Eq. 2.

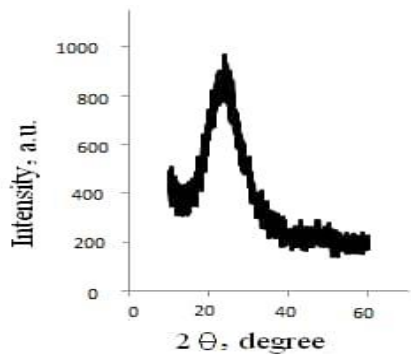
$$\text{Removal percentage} = (C_0 - C_e)/C_0 \times 100 \quad (2)$$

The dye concentration in different samples was measured Azure B using a Perkin Elmer Lambda UV spectrophotometer with a wavelength of 648 nm.

3. Results and discussion

3.1. Adsorbent characterizations

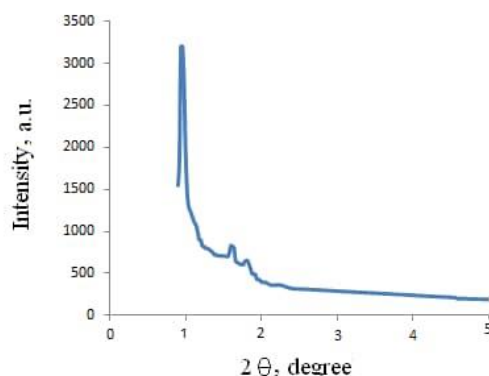
Fig. 2 illustrates an XRD spectrum of SSA and mesoporous SBA-15. The sample's reflection characteristics illustrate a single high-intensity peak followed by two smaller additional peaks, namely, the (100), (110), (200) in the region 0-3 2θ/degree, confirming the



(a)

symmetrical hexagonal structure (p6mm) of mesoporous SBA-15 (fig. 2b) (Guet al. 2010).

As shown in Fig. 2a, the XRD of extracted silica illustrates only a broad peak at 2θ=22, which is associated with amorphous silica and is extremely proper for easy dissolution in alkaline solutions to prepare a silicate solution.



(b)

Fig. 2. X-ray diffraction (XRD) spectrum of (a) SSA and (b) mesoporous SBA-15.

Morphology and microstructure of SBA-15 were assessed using SEM and TEM, respectively. The SEM image is presented in Fig. 3a. The Fig. 3a, exhibits structures including rods, spheres and a relatively uniform size of SBA-15 particles. The TEM image (Fig. 3b) of SBA-15 displayed that the sample was very porous, affirming the high mesoscopic order of the sample. This sample exhibited highly ordered pores which were hexagonally arranged with parallel channels, confirming the 2D (P6mm) structure of the sample. It is obvious that the mesoporous structure of SBA-15 was significantly consistent with the physisorption of nitrogen (N₂) and XRD results of small angle.

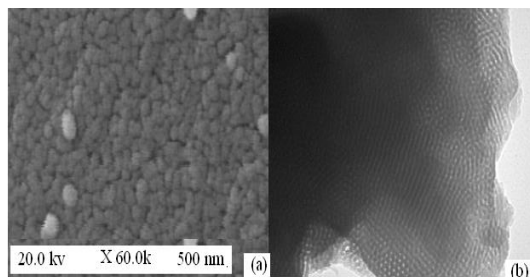


Fig. 3. (a) SEM and (b) TEM images of mesoporous SBA-15.

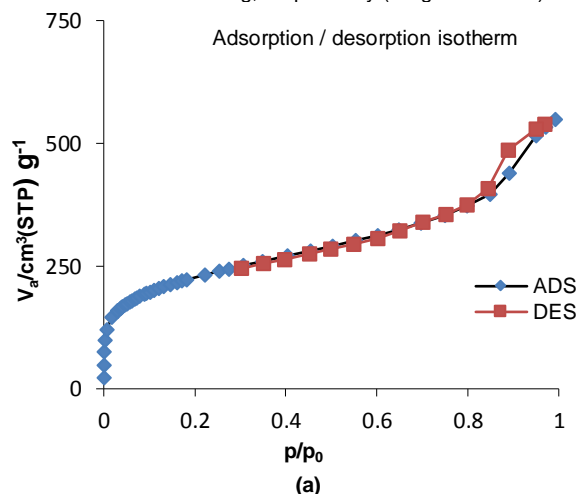
Fig. 4a represents the N₂ adsorption-desorption isotherm of pure silica SBA-15 at relative pressure (p/p₀) from 0.8 to 0.99 and BJH desorption pore distributions of mesoporous SBA-15 illustrate in Fig. 4b. The reason for the relatively sharp inflection can be due to capillary condensation (type IV isotherms), affirming the mesoporous structure of the sample. Moreover, the isotherm of SBA-15 demonstrated H4 hysteresis. Table 1 suggests the results of BET and BJH analysis. The average size of mesoporous pores of SBA-15 was 4.34 nm, which was in good line with the results of TEM (Kumaran et al. 2007).

Table 1. Structural parameters of mesoporous SBA- 15 obtained from nitrogen adsorption.

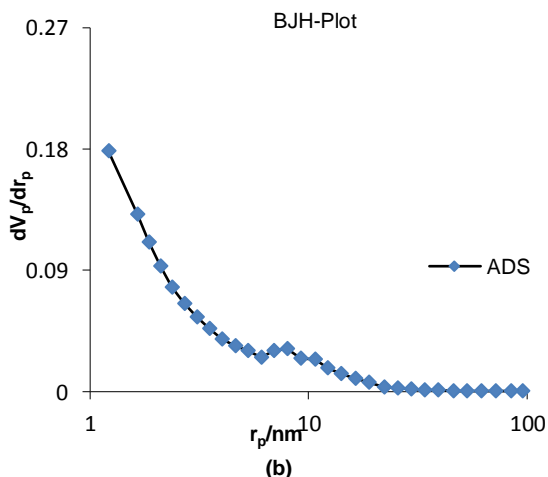
Materials	Total surface area, m ² /g	Mean Pore Diameter, nm	Total Pore Volume, mL/g	Primary mesopore Volume, mL/g
SBA-15	780	4.349	0.8483	0.66

BJH pore size distribution (b) of mesoporous SBA-15 Fig. 5 indicates the infrared spectra of the mesoporous SBA-15. The adsorption bands of SBA-15-based materials at 1100.17 cm⁻¹ and 880.26 1/cm were assigned to the Si-O-Si asymmetric and symmetric stretching vibration, respectively (Li et al. 2019). Besides, the adsorption band at about 980 cm⁻¹ was related to Si-OH bending vibration. The width of broad peak ranged from 3300 to 3550 1/cm

and band at 1629.27 1/cm were attributed to the asymmetric stretching vibration surface silanol groups (Si-OH) of physisorbed water molecules and bending, respectively (Xing et al. 2017).



(a)



(b)

Fig. 4. N₂ adsorption-desorption isotherms (a) and the corresponding BJH pore size distribution (b) of mesoporous SBA-15.

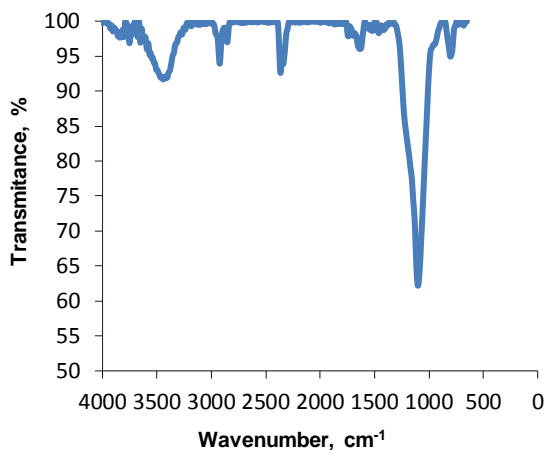


Fig. 5. FT IR spectra of prepared mesoporous SBA-15.

3.2. Evaluating the parameters affecting the adsorption process

3.2.1. The effect of contact time and dye initial concentration

Adsorption of Azure B on mesoporous SBA-15 was investigated by changing the initial concentration of dye in the test solution. To do so, 25 mL of dye solution with concentrations of 20, 30, 40, 60, 80 and 100 mg/L, initial pH of 5.5 and 0.01 g adsorbent were stirred at different contact times at 150 rpm and 25 °C. Fig. 6 illustrates that the adsorption capacity (q_e) increases with time, then reaches a constant value and more dye no longer removes from the solution. At this point, the amount of adsorbed dye on adsorbent was in dynamic equilibrium with the amount of desorbed dye from the adsorbent. Increasing the initial concentration of dye from 20 to 100 mg/L resulted in an increase of the adsorption capacity from 72.74 to 82.32 % for Azure B.

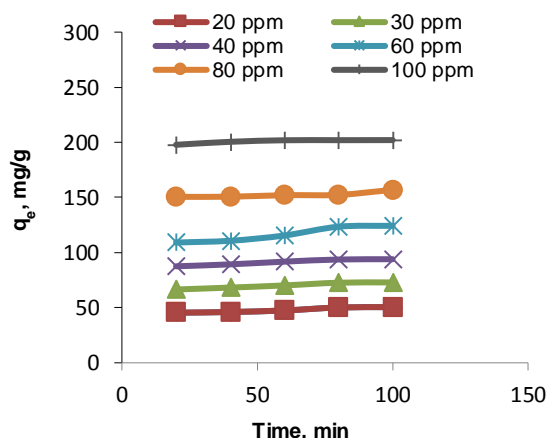


Fig. 6. Effect of contact time on Azure B adsorption (pH = 5.5, solution stirring rate = 150 rpm, adsorbent amount = 0.01g, temperature = 25 °C in different initial concentrations).

3.2.2. Effect of adsorbent amount on dye removal

Adsorption of Azure B on mesoporous SBA-15 was investigated by changing the amount of adsorbent in the test solution. For this purpose, 25 mL of dye solution with a concentration of 100 mg/L, initial pH of 5.5 and 0.003-0.09 g adsorbent were evaluated at 150 rpm and 25 °C for 30 minutes. Fig. 7 represents the Table percentage of dye removal based on increased adsorbent amount, and the results suggest that the maximum adsorption is achieved at 0.01 g adsorbent, leading to equilibrium. Obviously, the adsorption was enhanced by increasing the amount of adsorbent due to the enhanced adsorbent surface as well as more adsorption sites' availability. Therefore, 0.01 g adsorbent was selected as the optimum amount for subsequent experiments.

3.2.3. The effect of stirring rate of solution

The stirring rate of solution is an important parameter in adsorption phenomenon and affects the distribution of solutes in

soluble and adsorbent masses. In order to investigate the effect of stirring rate on adsorption amount, 25 mL dye solution with 100 mg/L concentration was stirred at various speeds of 90, 150 and 180 rpm.

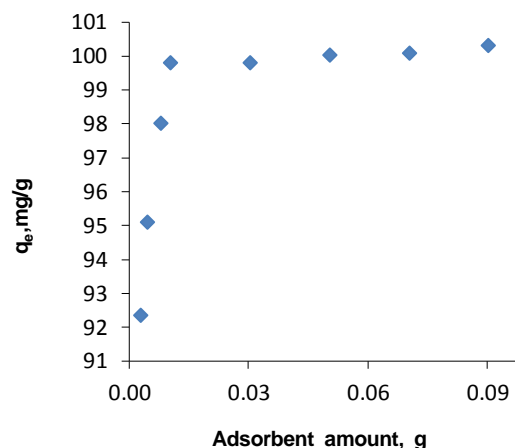


Fig. 7. Effect of adsorbent amount on dye removal (dye solution concentration = 100 mg/L, contact time = 30 min, pH = 5.5, solution stirring rate = 150 rpm, temperature = 25 °C).

The results are shown in Fig. 8. The stirring of the solution enhanced the transfer of the solutes from soluble masses to adsorbent sites, which resulted in the increase of adsorption rate. As the stirring speed elevates, the external mass transfer increases slowly.

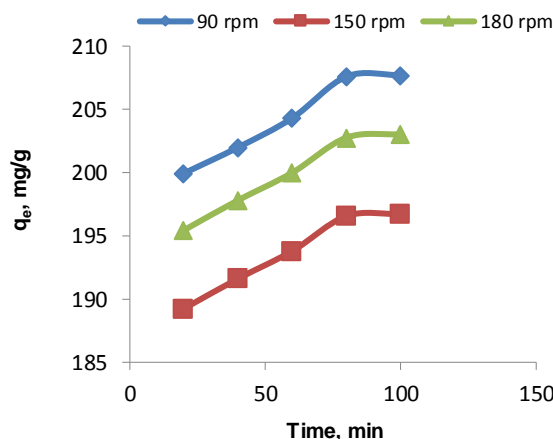


Fig. 8. Effect of stirring rate on Azure B adsorption (dye solution concentration = 100 mg/L, pH = 5.5, temperature = 25 °C).

3.2.4. Effect of temperature on dye removal

To determine the effect of temperature on adsorption amount, 25 mL of dye solution with 100 mg/L at different temperatures of 25, 45 and 65 °C was prepared. Fig. 9 displays the percentage of dye removal with growing temperature. Generally, the temperature has two effects on the adsorption process. Firstly, with the increase of temperature, the propagation rate of adsorbate molecules across the inner and outer layers of the adsorbent particles increases due to the decrease in the viscosity of the solution. Secondly, the equilibrium capacity of adsorbent is changed with increasing temperature for the adsorbates.

3.2.5. pH effect on dye removal

The pH of dye solution plays a key role in the adsorption process, in particular, adsorption capacity and affects the ionization degree of the materials present in the solution, surface charge of adsorbent, chemistry of dye solution and dissociation of functional groups on active sites of adsorbent. The effect of the pH on the adsorbed dye amount was investigated through changing pH in the range of 2-10.

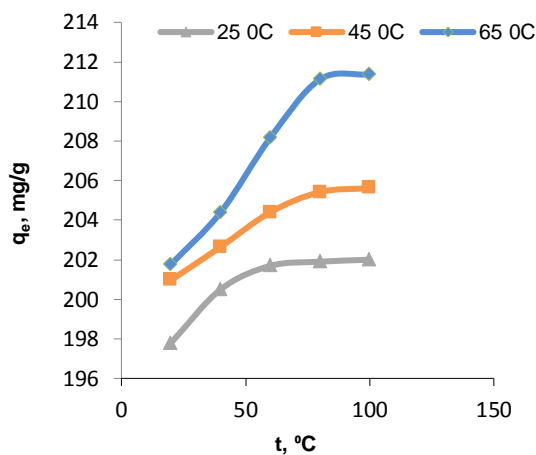


Fig. 9. Temperature effect on dye adsorption (dye solution concentration = 100 mg/ L, contact time = 30 min, pH = 5.5, solution stirring rate = 150 rpm).

As indicated in Fig. 10, the dye adsorption increases with rising pH from 2 to 8 and then does not increase significantly. At low pH, the surface charge of adsorbent was positive; as a result, the cationic dyes were not adsorbed due to the electrostatic repulsion, and the effective competition between H⁺ ions and dye cations reduced the adsorbed dye amount. At high pH, the surface charge of adsorbent was negative; as a result, the adsorbed dye amount was increased due to the electrostatic attraction force of the dye cationic molecules and negative charge surface of the adsorbent.

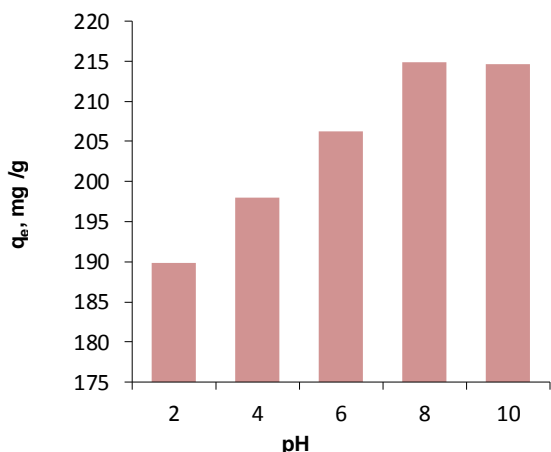


Fig. 10. Effect of pH on adsorption of Azure B. Conditions: dye solution concentration=100 mg/L, contact time = 80 min, solution stirring rate = 90 rpm, temperature = 65 °C.

3.3. Adsorption equilibrium isotherms

The purpose of adsorption isotherms is to establish a relationship between the adsorbate concentration in the adsorbed amount and solution during the interactions between adsorbent and adsorbate. Adsorption data in this study are described with Langmuir, Freundlich and Temkin adsorption isotherm models. An adsorption isotherm is identified with a series of certain constants so that the constant values obtained for each isotherm express the surface properties as well as the tendency of adsorbent and adsorbate. The linear form of the Langmuir (3) and Freundlich (4) equations is represented as:

$$(1/(q_{max} K_L)) + (1/q_{max})C_e = C_e/q_e \tag{3}$$

$$\ln q_e = \ln K_f + (1/n_f) \tag{4}$$

The adsorption data are illustrated in Table 2 with the linear form of the Langmuir and Freundlich isotherm. The linear plot of C_e/q_e versus C_e gives K_L is the slope and q_{max} is the intercept as the results for Langmuir isotherm (Fig. 11).

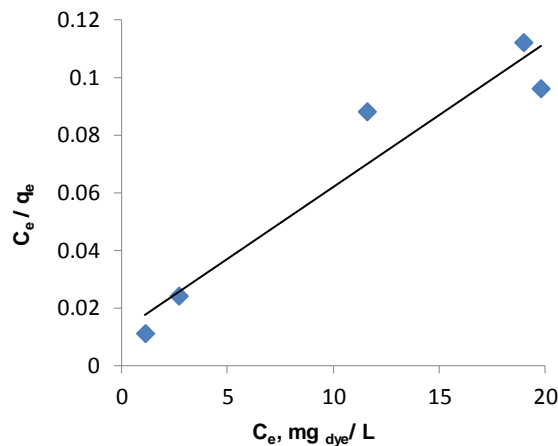


Fig. 11. Langmuir isotherm surface adsorption in adsorbing Azure B by SBA-15.

To study the Freundlich isotherm and calculate K_F and 1/n_f values based on intercept and slope, the plot of lnq_e versus lnC_e was drawn (Fig. 12). Higher K_F values indicate a greater adsorption tendency of adsorbate toward adsorbent, and 1/n_f is a heterogeneity factor expressing the adsorption intensity. The values obtained for K_F and 1/n_f are displayed in the Table 2.

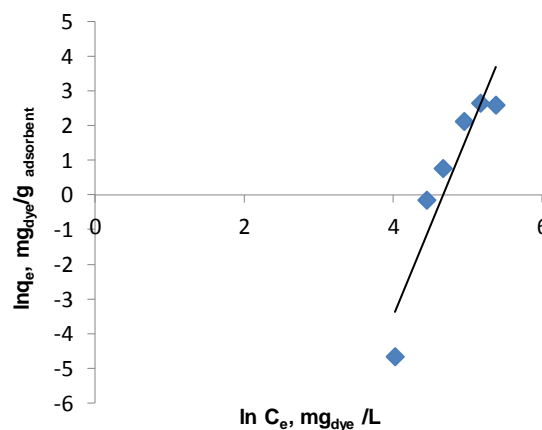


Fig. 12. Freundlich isotherm surface adsorption in adsorbing Azure B by SBA-15.

Table 2. Modeling results of adsorption isotherms of dye Azure B on mesoporous SBA-15 mesoporous SBA-15 obtained from nitrogen adsorption.

Isotherms	Parameters
Langmuir	
q _{max} , mg/g	166.66
K _L	0.6
R ²	0.978
Freundlich	
n _f	5.31
K _F	85.62
R ²	0.946
Temkin	
K _T , L/g	93.70
B	2.112
R ²	0.954

On the other hand, the interactions between adsorbent and adsorbate are clearly shown by a factor of Temkin isotherm. Through ignoring the very large and low value of concentrations, the Temkin model presumes that the adsorption heat (function of temperature) of all molecules in the layer would reduce linearly than logarithmic with coverage (Tsai et al. 2016). The linear form of this isotherm model is as follows (5):

$$q_e = B \ln A + B \ln C_e \tag{5}$$

where, A is the equilibrium binding constant corresponding to the maximum binding energy (L/g), B = RT/b, b is the Temkin constant

related to heat of sorption (J/mol), T is the absolute temperature (K) (Tsai et al. 2016) and R is the gas constant (8.314 J/mol K).

According to the results of Table 2, it can be stated that due to the higher squared correlation coefficient (R²) obtained for the Langmuir isotherm than that for the Freundlich isotherm, the equilibrium adsorption data follow the Langmuir isotherm well; therefore, the single coat of Azure B layer affects mesoporous particles and confirms the homogeneous distribution of active sites on the adsorbent.

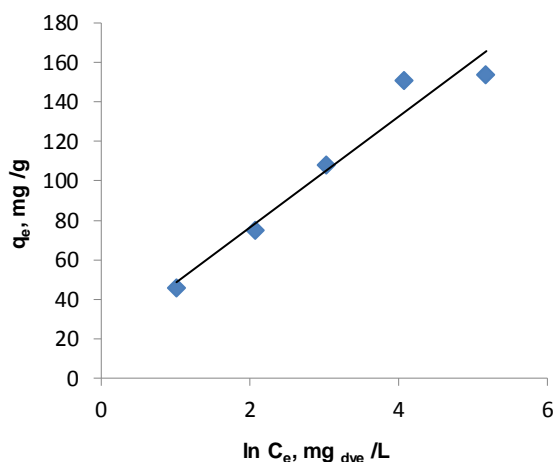


Fig. 13. The Temkin isotherm plot for Azure B dye adsorption on mesoporous SBA-15.

3.3.1. Comparing the findings of this study with other studies

Evaluating different isotherms in the ongoing study demonstrated that the Langmuir isotherm was the most suitable isotherm to explain the adsorption process; hence, the value of q_{max} = 166 mg/g taken from the above calculations was compared with that gained from other results of other studies in Table 3. In this Table, by examining the q_{max} obtained from adsorbents originating from agricultural wastes such as activated carbon of rice ash and palm leaf, it is observed that the value of q_{max} in the present study, i.e. the SBA-15 synthesized by sweep ash is higher. Moreover, the maximum adsorption gained by this adsorbent was comparable to synthesized adsorbents such as Ni-SBA with tetraethoxysilane as the industrial silica source. On the other hand, Table 4 illustrates a comparison between the adsorption of different dyes such as Janus Green B, Methylene blue and so on and that of SBA-15 adsorbent. By examining the adsorption of different industrial dyes on the SBA-15 substrate, it was observed that the synthesized SBA-15 in the present study had a significant adsorption capacity for Azure B molecules, and the uniform distribution of active sites on it responded well to adsorption and interaction of Azure B particles.

Table 3. Comparison of adsorption performance of mesoporous SBA-15 for Azure B adsorption with other adsorbents.

Adsorbent	Adsorption capacity, mg/g	References
Rice husk activated carbon	144.93	Duraisamy et al. 2015
Palm leaf	41.49	Zhu et al. 2014
Raw KT38 kaolin	52.8	Mouni et al. 2018
Ti-SBA-15	208.3	Qiang et al. 2019
CNTs/Zn:ZnO@Ni ₂ P-NCs	38.6	Alipanahpour et al. 2019
SBA-15	166.6	This work

3.4. Adsorption thermodynamics

The effect of temperature on the adsorption process of the Azure B solution with adsorbent dosage of 0.01 g/L at pH=8 was assessed at different temperatures of 25, 45 and 65°C. The study of thermodynamic parameters such as Gibbs free energy (ΔG°), enthalpy change (ΔH°) and entropy change (ΔS°) illustrated the possibility of performing the adsorption process. The van't Hoff equation was applied to gain the value of these parameters, (Eq. 6) (Aharoni and Ungarish. 2016).

$$\log q_e/C_e = \Delta S^\circ/2.303 R + (-\Delta H^\circ)/2.303 R \quad (6)$$

$$\Delta H^\circ = \Delta G^\circ - T \Delta S^\circ$$

The acquired values of ΔH°, ΔS° and ΔG° are presented in Table 5.

Table 4. Comparison between the adsorption of different dyes on mesoporous SBA-15.

Adsorbents	Dyes	Q _{max} , mg/g	Reference
SBA-15	Methylene blue	49.26	Huang et al. 2011
SBA-15	Janus Green B	66.44	Yanling et al. 2010
SBA-15	Methylene blue	280	Yanling et al. 2010
SBA-15	Methyl violet dye	9.4	Nesic et al 2019
SBA-15	Brilliant green	119	Asif et al. 2019
SBA-15	Azure B	166.6	This work

Table 5. Thermodynamic parameters for Azure B adsorption on mesoporous SBA-15.

Temperature, K	ΔG°, J/mol	ΔH°, J/mol	ΔS°
338	-7191.3		
318	-6445.72	5409.32	37.28
298	-5855.08		

Negative changes in the Gibbs free energy indicate that the adsorption process is spontaneous, and the positive standard enthalpy changes display that the reaction is endothermic. On the other hand, the positivity of the standard entropy changes in the system illustrates an increase of disorder in the solid-solution interface.

3.5. Adsorption kinetics and mechanism determination

To determine the dye adsorption rate, the linear form of pseudo-first and second-order kinetic equations was used. The results of the performed experiments in optimum conditions and the amount of Azure B (mg/g) adsorbed on the adsorbent at any moment are presented in Table 6. These results indicated that the adsorption of Azure B was balanced at all concentrations after 80 min. The plot of Log (q_e-q_t) versus t is shown in Fig. 14 to examine the pseudo-first-order mechanism. This plot was nonlinear and the calculated q_e values (q_{e,cal}) of this kinetic model were much lower than the experimental q_e values (q_{e,exp}); hence, the adsorption process did not follow the pseudo-first-order kinetics; as a result, the propagation process through the boundary layer did not control the rate of the adsorption process. According to Table 6, the low values of the correlation coefficient confirm that the adsorption process does not follow the pseudo-first-order kinetic model.

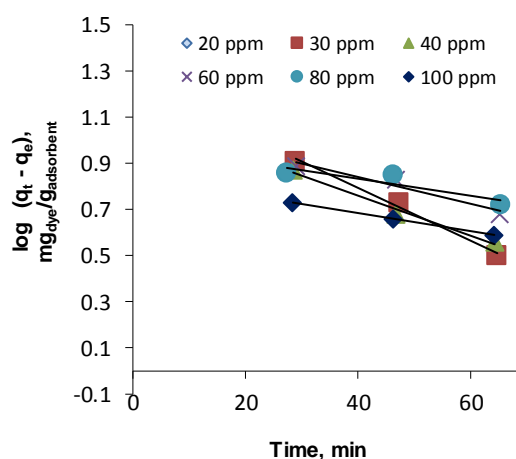


Fig. 14. Pseudo-first-order rate of Azure B adsorption by SBA-15.

The pseudo-second-order rate constants K₂ and q_e were obtained based on intercept and slope, respectively, the plot of t/q_e versus t was drawn (Fig. 15). These values and line's R² are reported in Table 6. The very good agreement of the calculated q_e values (q_{e,cal}) with the experimental values q_e (q_{e,exp}) and the line obtained with high R² indicated that Azure B adsorption on SBA-15 followed the

pseudo-second-order kinetic model and chemical interactions controlled the rate of the adsorption process.

Table 6. Comparison of kinetic constants of pseudo-first- and – second-order kinetic models for Azure B adsorption on mesoporous SBA-15.

Pseudo-second-order rate		
R ²	q _e , mg/g	K ₂ , g/mg h
0.999	250	2.28×10 ⁻³
Pseudo-first-order rate		
R ²	q _e , mg/g	K ₂ , g/mg h
0.864	38.9	0.041

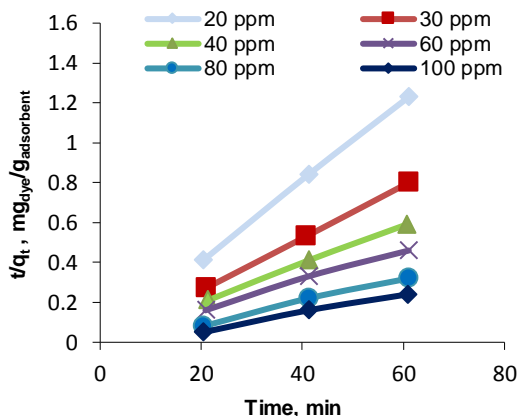


Fig. 15. Pseudo-second-order rate of Azure B adsorption.

3.5. Desorption and regeneration studies

A good adsorbent must demonstrate good regenerative capacity for multiple uses in addition to excellent adsorption. In order to investigate the maximum desorption efficiency, the Azure B desorption was initially evaluated by adjusting 10 mL of 0.1 mg/mL Azure B at pH = 8 and was dispersed after adding 20 mg of mesoporous SBA-15 for 24 hours. After adsorption, the saturated mesoporous SBA-15 was removed and placed in 10 mL of deionized water. The pH value of the system was adjusted to 1 for desorption. The Azure B concentration was measured by the UV-V is spectrometer every 10 minutes for 2.30 hours. In other words, electrostatic repulsion can play an important role in the process of adsorption and desorption at pH = 1.

Fig. 16 exhibits the results of the studies on desorption. The results suggested that after six periods of the absorption-desorption process, when the time reached 130 min, the Azure B desorption efficiency was about 94.98 %, indicating the good reusability of the SBA-15 nano particle for absorbing the cationic dye Azure B.

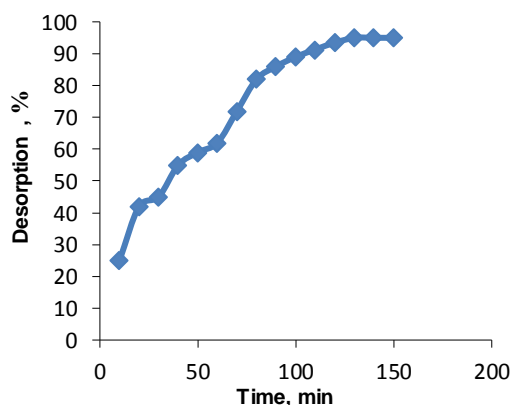


Fig. 16. Desorption efficiency for Azure B on mesoporous SBA-15 (Concentration of Azure B and adsorbent are maintained at 0.1 mg/mL and 2 g/L at 298 K, respectively).

4. Conclusions

According to the present study, the SBA-15 as a good, green and inexpensive adsorbent with high adsorption capacity (166.6 mg/g) is highly effective in absorbing Azure B dye. Experimental data suggest that the adsorption capacity depends on variables such as pH, temperature, stirring rate, adsorbent amount, contact time and initial

dye concentration. The linearity of the plot of t/q versus t with high R^2 and the proximity of the calculated q_e values and experimental q_e revealed the pseudo-second-order model which was provided the best fit to the experimental data, demonstrating that a chemisorption mechanism takes part in the adsorption process. The study of equilibrium experimental data based on Langmuir, Freundlich and Temkin isotherms indicated that the Langmuir model had better match with experimental data compared to other models. According to thermodynamic studies, the adsorption process of Azure B on the synthesized SBA-15 is endothermic and spontaneous.

Acknowledgments

The authors would like to thank the University of Mazandaran, Iran, providing facilities for the present study.

References

- Abo-Farha S.A., Comparative study of oxidation of some azo dyes by different advanced oxidation processes: Fenton like photo-fenton and photo-fenton-like, *The Journal of American Science* 6 (2010) 128-42.
- Alipanahpour D.E., Ghaedi M., Asfaram A., Mehrabi F., Sadeghfard F., efficient adsorption of Azure B on to CNTs/Zn: ZnO @ Ni₂P-NCs from aqueous solution in the presence of ultrasound wave based on multivariate optimization, *Journal Of Industrial and Engineering Chemistry* 74 (2019) 55–62.
- Asif J.K., Jinxi S., Khalid A., Fozia R., Mesoporous silica MCM-41, SBA-15 and derived Bridged polysilsesquioxane SBA-PMDA 1 for the selective removal of textile reactive dyes from wastewater, *Journal of Molecular Liquids* 298 (2019) 1-10.
- Azizi S.N., Ghasemi S., Kavian S., Synthesis and characterization of NaX nanozeolite using stem sweep as silica source and application of Ag-modified nanozeolite in electrocatalytic reduction of H₂O₂, *Biosensors and Bioelectronics* 62 (2014) 1-7.
- Azizi S.A., Ghasemi S., Chiani E., Nickel/mesoporous silica (SBA-15) modified electrode: An effective porous material for electrooxidation of methanol, *Electrochimica Acta* 88 (2013) 463–472.
- Belessi V., Romanos G., Boukos N., Lambropoulou D., Trapalis C., Removal of reactive Red 195 from aqueous solutions by adsorption on the surface of TiO₂ nanoparticles, *Journal of Hazardous Materials* 170 (2009) 836–844.
- Daneshvar N., Salari D., Khataee A.R., Photocatalytic degradation of azo dye acid red 14 in water: investigation of the effect of operational parameters, *Journal of Photochemistry and Photobiology A: Chemistry* 157 (2003) 111-116.
- Duraisamy R., Kiruthigam P., Hirpaye B., Berekute A., Adsorption of azure B dye on rice husk activated carbon: equilibrium, kinetic and thermodynamic studies, *International Journal of Water Research* 5 (2015) 18-28.
- Ghadiri S., Nabizadeh R., Mahvi A., Nasserli S., Kazemian H., Mesdaghinia A., Methyl tert-butyl ether adsorption on surfactant modified natural zeolites, *Iranian Journal of Environmental Health Science & Engineering* 7 (2010) 241-252.
- Gök Ö., Özcan A.S., Özcan A., Adsorption behavior of a textile dye of Reactive Blue 19 from aqueous solutions onto modified bentonite, *Applied Surface Science* 256 (2010) 5439-5443.
- Gu X., He M., Shi Y., Li Z., La-containing SBA-15/H₂O₂ systems for the microwave assisted oxidation of lignin model phenolic monomer, *Maderas-Cienciy Tecnologia* 12 (2010) 181-188.
- Huang C.H., Chang K.P., Ou H.D., Chiang Y.C., Wang C.F., Adsorption of cationic dyes onto mesoporous silica, *Microporous Mesoporous Mater* 141 (2011) 102–109.
- Kalopathy U., Proctor A., Shultz J., A simple method for production of pure silica from rice hull ash, *Bioresource Technology* 73 (2000) 257-262.
- Kikuchi R., Application of coal ash to environmental improvement transformation into zeolite, potassium fertilizer and FGD absorbent, *Resources Conservation and Recycling* 27 (1999) 333-346.

- Kumaran G.M., Garg S., Soni K., Kumar M., Sharma L.D., Rao K.S.R., Dhar G.M., Effect of Al-SBA-15 support on catalytic functionalities of hydrotreating catalysts, II effect of variation of molybdenum and promoter contents on catalytic functionalities, *Industrial & Engineering Chemistry Research* 46 (2007) 4747-475.
- Kyzas G.Z., Lazaridis N.K., Mitropoulos A.C., Removal of dyes from aqueous solutions with untreated coffee residues as potential low-cost adsorbents: equilibrium, reuse and thermodynamic approach, *Chemical Engineering Journal* 189 (2012) 148-59.
- Li X., Zhang J., Liu B., Liu J., Wang C., Chen G., Hydrodeoxygenation of lignin-derived phenols to produce hydrocarbons over Ni/Al-SBA-15 prepared with different impregnants, *Fuel* 243 (2019) 314-321
- Lotito M., De Sanctis M., Di Iaconi C., Bergna G., Textile wastewater treatment: aerobic granular sludge vs activated sludge systems, *Water Research* 54 (2014) 337-346.
- Mouni L., Belkhirri L., Bollinger G.C., Bouzaza A., Assadi A., Tirri T., Dahmoune F., Madani K., Remini H., Removal of methylene blue from aqueous solutions by adsorption on Kaolin: kinetic and equilibrium studies, *Applied Clay Science* 153 (2018) 38- 45.
- Muhammad A., Shafeeq A., Butt M.A., Rizvi Z.H., Chughtai M.A., Rehman S., Decolorization and removal of COD and BOD from raw and biotreated textile dye bath effluent through advanced oxidation processes (AOPS), *Brazilian Journal of Chemical Engineering* 25 (2008) 453-459.
- Nesic A.R., Kokunesoski M.J., Volkov-Husovic T.D., Sava J.V., New method for quantification of dye sorption using SBA mesoporous silica as a target sorbent, *Environmental Monitoring and Assessment* 188 (2016) 160-172.
- Qiang T., Song Y., Zhao J., Li J., Controlled incorporation homogeneous Ti-doped SBA-15 for improving methylene blue adsorption capacity, *Journal of Alloys and Compounds* 770 (2019) 792-802.
- Speybroeck M.V., Barillaro V., Thi T.D., Mellaerts R., Martens J., Humbeek J.V., Vermant J., Annaert P., Mooter G.V., Augustijns P., Ordered mesoporous silica materials SBA-15: A broad spectrum formulation platform for poorly soluble drugs, *Journal of Pharmaceutical Sciences* 98 (2008) 2648-2658.
- Tsai C.H., Chang W.C., Saikia D., Wu C.E., Kao H.M., Functionalization of cubic mesoporous silica SBA-16 with carboxylic acid via one-pot synthesis route for effective removal of cationic dyes, *Journal of Hazardous Materials* 309 (2016) 236-248.
- Thuadaj N., and Nuntiya A., Preparation of nanosilica powder from rice husk ash by precipitation method, *Chiang Mai Journal of Science* 35 (2008) 206-211.
- Ulrich K., Galvosas P., Karger J., Grinber F., Vernimmen J., Meynen V., Cool P., Self-Assembly and diffusion of block copolymer templates in SBA-15 nanochannels, *Journal of Physical Chemistry B* 114 (2010) 4223-4229.
- Xiangping Li., Han Y., Jianguang, Zhang., Juping, L., Guanyi, C., Effect of organic template removal approaches on physicochemical characterization of Ni/Al-SBA-15 and eugenol hydrodeoxygenation, *Journal of Solid State Chemistry* 282 (2019) 121063
- Xiao L.P., Li J.Y., Jin H.X., Xu R.R., Removal of organic templates from mesoporous SBA-15 at room temperature using UV/dilute H₂O₂, *Microporous and Mesoporous Materials* 96 (2006) 413-418.
- Yanling D., Bin L., Shuying Z., Jingxiang Z., Xiaoguang W., Qinghai C., Removal of methylene blue from coloured effluents by adsorption onto SBA-15, *Nanomaterials* 86 (2010) 616-619.
- Zhu G.Q., Wang F.G., Xu K.J., Ga Q.C., Li Y.Y., Structure and properties of carboxymethyl chitosan film modified by poly(l-lactic acid), *Asian Journal of Chemistry* 26 (2014) 33-35.